

New quasicrystals of alloys containing s , p , and d elements

H. S. Chen, J. C. Phillips, P. Villars,* A. R. Kortan, and A. Inoue[†]
AT&T Bell Laboratories, Murray Hill, New Jersey 07974

(Received 5 March 1987; revised manuscript received 20 April 1987)

New quasicrystals are obtained in alloys containing s , p , and d elements (so-called PSD alloys): AuLi_3Al_6 , $\text{Zn}_{17}\text{Li}_{32}\text{Al}_{51}$, $\text{Ga}_{16}\text{Mg}_{32}\text{Zn}_{52}$, and $\text{Ag}_{15}\text{Mg}_{35}\text{Al}_{50}$. Transmission electron microscopy and x-ray diffraction studies reveal that these PSD quasicrystals exhibit a unique peak-intensity modulation and packing density suggesting similar atomic decorations of the rhombohedron unit cells of three-dimensional Penrose tiling.

Since the first report of an icosahedral (i) phase in melt-spun Al_6Mn ,¹ the i phase has been found in melt-spun Al-Mn, -Cr, -Fe, -V, -W, . . . , Al-Si-Mn, $\text{Mg}_3\text{Zn}_3\text{Al}_2$, Mg_4CuAl_6 , and $(\text{Ti},\text{V})_2\text{Ni}$. A stable ternary compound of $\text{Al}_6\text{Li}_3\text{Cu}$, formerly designated as T_2 phase by Hardy and Silcock,² has been found to exhibit an icosahedral quasicrystalline structure.³ Most of the i phases are observed to exist in composition ranges where equilibrium phases are of the Frank-Kasper type in which icosahedral coordination shells dominate in the structure. Thus the formation of the icosahedral quasicrystals is closely related to the structure of the equilibrium state.⁴ Recently, Villars, Phillips, and Chen⁵ have utilized quantum structural diagrams developed to describe stable crystalline compounds to ternary quasicrystals. Their analysis predicted many possible new quasicrystals of the $A_{15}B_{35}C_{50}$ type, where A (or C) is a p element (such as Al, Ga, Ge, or Sn), B is an s element (such as Li, Na, or Mg), and C (or A) is a near noble metal or d element (such as Ni, Cu, Ag, Au, or Zn). Crystalline compounds of these so-called PSD- (or DSP) type alloys have the (cI 162)-structure type and are distinguishable from the other best-known quasicrystal-forming alloys, Al-TM, which are based on the (cP 138) structure of $\text{Al}_9\text{Mn}_2\text{Si}_2$. Here TM is a transition metal. We have made preliminary studies of Li- and Mg-containing alloys listed in Ref. 5 and found a number of new quasicrystals. These new quasicrystals, revealed by transmission electron microscopy (TEM) and x-ray diffraction, show distinct structural features as compared with the Al-TM alloy system.

PSD-type alloys were prepared by induction melting of high-purity elements in a pyrolytic boron-nitride crucible under an argon atmosphere. Thin ribbons of about 1-mm width and 30- μm thickness were produced by melt spinning with a copper wheel ~ 20 -cm diameter rotating at 2000 rpm in an enclosed argon atmosphere. Both the as-cast alloys and melt-spun ribbons were powdered for x-ray diffraction. X-ray diffraction measurements were done using a Philips APD 6300 automatic diffractometer with Cu $K\alpha$ radiation. The instrumental resolution was $\sim 2.3 \times 10^{-3} \text{ \AA}^{-1}$ half width at half maximum (HWHM). The samples were scanned between 10° to 110° in 2θ with a step size of 0.05° . The melt-spun ribbons had several thin areas which were transparent to electrons, and consequently were examined by TEM without further preparation. The specimens were exam-

ined with a Philips EM 420 transmission microscope.

The melt-spun specimens show the typical rosette microstructure of icosahedral crystals, as exemplified for AuLi_3Al_6 and $\text{Ag}_{15}\text{Mg}_{35}\text{Al}_{50}$ in Fig. 1. The coral-like fingers of each rosette extend from the rosette center or nucleus radially outward. Between branches and grain boundaries a cubic phase R ($a = 14.00 \text{ \AA}$) or fcc Al precipitates respectively in Au-Li-Al or in Ag-Mg-Al. Very often the R phase has been found to have a very definite orientational relationship to the i phase. As seen in Fig.

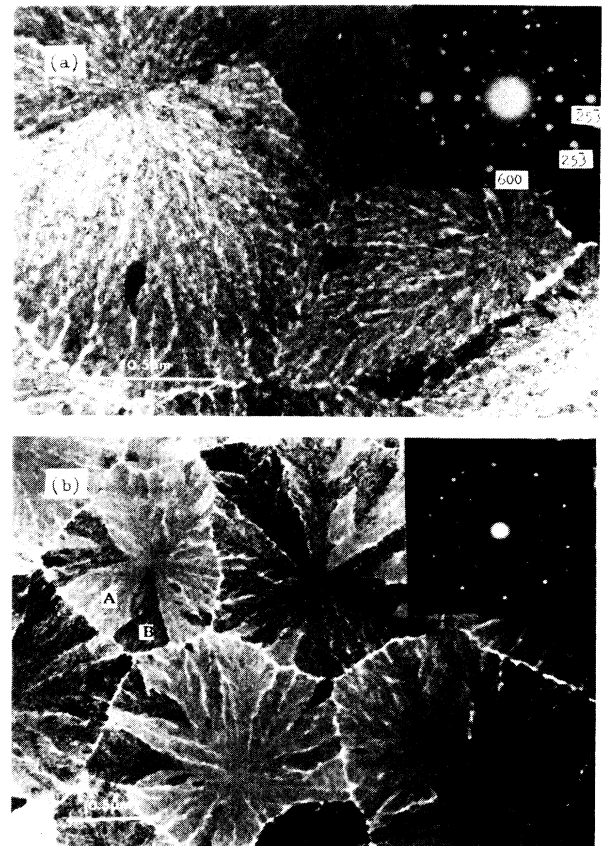


FIG. 1. Transmission electron microscope micrographs and diffraction patterns along fivefold axis of (a) AuLi_3Al_6 and (b) $\text{Ag}_{15}\text{Mg}_{35}\text{Al}_{50}$.

1(a), a fivefold icosahedral symmetry axis coincides closely with $\langle 035 \rangle$ -type zone axes of the cubic *R* grains. Furthermore, the bright $\langle 532 \rangle$ - and $\langle 600 \rangle$ -type spots nearly coincide with the 221 001-type icosahedral spots. The definite orientational relationship between the icosahedral crystal and surrounding cubic grains has been seen previously in Al-Si-Mn alloys,⁶ indicating a strong structural relation between these two phases. We have occasionally found a nodule type of icosahedral grain in Ag-Mg-Al with pie-shaped sectors, e.g., *A* and *B*, having a different orientation [Fig. 1(b)]. These nodules are somewhat similar to those observed in the *i* phase of $\text{Al}_{73}\text{Si}_{13}\text{Mn}_{14}$,⁷ and of $\text{Mg}_{32}(\text{Al,Zn})_{49}$ by Ramachandrarao and Sastry.⁴ There appeared to be no specific orientational correlation between these sectors.

X-ray diffraction studies revealed that among all the cast alloys prepared, only the Cu-Li-Al was found to contain an *i* phase. We found that replacing Cu with either Au or Ag enhanced the formation of the cubic *R* phase. For example, melt-spun AgLi_3Al_6 even by melt spinning was found to be single *R* phase, and the as-cast AuLi_3Al_6 was found to consist of two phases, the *R* phase and an unidentified crystalline phase.

Icosahedral quasicrystals were observed in melt-spun AuLi_3Al_6 , $\text{Zn}_{17}\text{Li}_{32}\text{Al}_{51}$, $\text{Ga}_{16}\text{Mg}_{32}\text{Zn}_{52}$, $\text{Ag}_{15}\text{Mg}_{35}\text{Al}_{50}$, $\text{Al}_2\text{Mg}_3\text{Zn}_3$, $\text{Cu}_9\text{Mg}_{37}\text{Al}_{54}$, and $\text{CuLi}_3\text{Al}_{5.9}$. Preliminary results for the Ga-Mg-Zn and Al-Mg-Zn alloys have been reported previously.⁸ Figure 2 shows powder x-ray diffraction patterns of some of the icosahedral crystals. Also shown in Fig. 2 for comparison is that of $\text{Al}_{74}\text{Si}_6\text{Mn}_{15}\text{Fe}_5$. Here we use the indexing scheme of Elser.⁹ The $\text{CuLi}_3\text{Al}_{5.9}$ alloy [Fig. 2(a)] consists mostly of an *i* phase and of a considerable amount of fcc Al. This indicates that the *i* phase contains less Al than the previously suggested compound CuLi_3Al_6 . The detailed compositional dependence of an *i* phase in Cu-Li-Al alloys will be reported elsewhere.¹⁰ The AuLi_3Al_6 alloy [Fig. 2(b)] consists of *i* and *R* phases, while the diffraction pattern of the $\text{Zn}_{17}\text{Li}_{32}\text{Al}_{51}$ [Fig. 2(c)] is similar to that of $\text{CuLi}_3\text{Al}_{5.9}$ consisting of *i* and fcc Al phases. The Mg-containing alloys, $\text{Ag}_{15}\text{Mg}_{35}\text{Al}_{50}$, $\text{Ga}_{16}\text{Mg}_{32}\text{Zn}_{52}$, and $\text{Al}_2\text{Mg}_3\text{Zn}_3$, exhibit similar diffraction patterns which could be indexed with a single *i* phase as exemplified for the Ag-Mg-Al alloy in Fig. 2(d) (also see Fig. 2 of Ref. 8). The peak positions observed are in good agreement with the calculated values within 0.2%.

The normalized integrated intensities I_r ($=I/I_{221001}$) (Ref. 11) and half widths at half maximum, ΔQ , are listed in Table I, where $Q_r = |Q|/|Q_{221111}|$. The calculated rhombohedral edge length a_R (e.g., $\approx 13.308/|Q_{221111}|$) (Ref. 9) is also listed in the table. Figure 3 illustrates the integrated peak intensities $I_r(Q_r)$ of the icosahedral crystals. Previously reported data⁸ for $\text{Ga}_{16}\text{Mg}_{32}\text{Zn}_{52}$, $\text{Al}_2\text{Mg}_3\text{Zn}_3$, $\text{Al}_{60}\text{Si}_{20}\text{Cr}_{20}$, and $\text{Al}_{74}\text{Si}_6\text{Mn}_{20}$ are also shown in Fig. 3, where alloys of Li-based, Mg-based, and Al-TM are grouped into three distinct types and denoted by the symbols \circ , Δ , and \bullet , respectively. The asterisk (*) in Fig. 3 refers to the normalization point. As seen in Table I and Fig. 3 the peak intensities of the PSD-type (Li-based and Mg-based) icosahedral crystals are qualitatively different from those of the Al-TM type. In particular the 111 100,

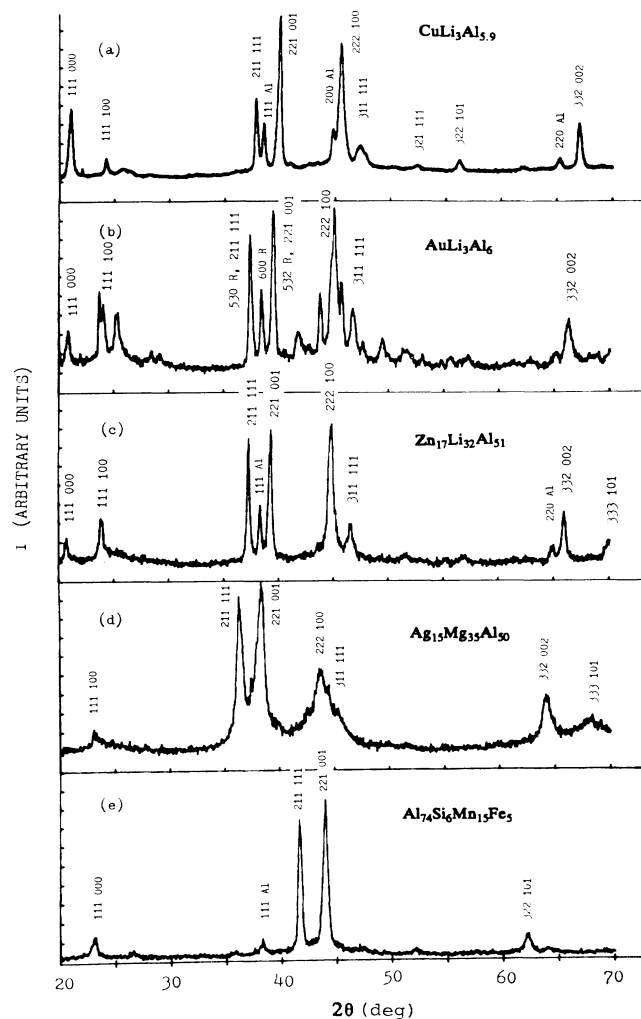


FIG. 2. X-ray powder diffraction patterns of melt-spun (a) $\text{CuLi}_3\text{Al}_{5.9}$, (b) AuLi_3Al_6 (all unindexed peaks belong to the *R* phase), (c) $\text{Zn}_{17}\text{Li}_{32}\text{Al}_{51}$, (d) $\text{Ag}_{15}\text{Mg}_{35}\text{Al}_{50}$, and (e) $\text{Al}_{74}\text{Si}_6\text{Mn}_{15}\text{Fe}_5$.

222 100, 311 111, 333 101, and 422 211 peaks, which are barely observable in the *i*-Al-TM alloys, are very strong in the PSD alloys, while the reverse holds for the 322 101 peak. The present results suggest that the PSD-type and the Al-TM-type quasicrystals have the same icosahedral three-dimensional Penrose tilings (3DPT) but different decoration of rhombohedral unit cells. Knowles and Stobbs¹² demonstrate that the computed intensities of diffraction patterns from model structures of 3DPT are very sensitive to the atomic decoration of the underlying rhombohedron unit cells. It is believed that in the PSD system the heavy atoms of *p* and *d* elements decorate the edges of the 3DPT, while in the Al-TM system the heavy TM metals occupy the vertices of these basic units that make up the icosahedral structure.¹³

Henley and Elser¹³ concluded from their structural models that the ratio $a_R/\bar{d}=2.0$ for alloys of the (Al,Zn)Mg type, and $a_R/\bar{d}=1.65$ for alloys of the Al-Si-Mn-type, where a_R is the icosahedral lattice parameter

TABLE I. The normalized peak intensity I_r and HWHM ΔQ (10^{-2} \AA^{-1}) of icosahedral crystals. The lattice parameter a_R (\AA) is shown in parenthesis.

Index	Q_r	Cu-Li-Al (5.035)		Zn-Li-Al (5.111)		Au-Li-Al (5.107)		Ag-Mg-Al (5.229)		Al-Si-Mn-Fe (4.590)	
		I	ΔQ	I	ΔQ	I	ΔQ	I	ΔQ	I	ΔQ
110000	0.402	6	1.2	5	3.3	5	1.4
111000	0.563	44	1.4	17	1.8	23	1.8	11	2.4
111100	0.650	10	0.7	33	1.1	38	0.6	12	2.6
211111	1.000	46	1.1	89	0.8	84	0.8	92	1.2	83	1.4
221001	1.052	100	1.0	100	1.2	100	1.2	100	2.1	100	1.9
222100	1.193	79	0.8	110	1.9	99	1.6	42	2.6
311111	1.236	13	2.2	38	1.8	16	2.2	3	3.0
321111	1.358	3	1.6	5	3.7	3	2.9
322101	1.451	6	1.2	4	2.4	6	1.6	11	2.5
322111	1.487	5	3.4	8	1.6	3	2.7
332002	1.701	28	0.9	36	2.2	28	2.4	31	2.6	36	2.1
333101	1.792	4	1.5	15	2.0	20	1.8	15	3.1
422211	1.821	7	1.6	15	1.8	11	2.0	9

and \bar{d} is the average interatomic spacing of atoms in corresponding crystalline compounds. Since \bar{d} values are not easily accessible, we take the average Goldschmidt atomic diameter, \bar{a} , to plot against the i -phase lattice parameter a_R in Fig. 4. The values of a_R reported by Inoue, Kimura, and Masumoto¹⁴ for $\text{Al}_{82.5}\text{V}_{17.5}$ (4.75 \AA), $\text{Al}_{84.6}\text{Cr}_{15.4}$ (4.65 \AA), and $\text{Al}_{77.5}\text{Mn}_{22.5}$ (4.58 \AA) are also shown in Fig. 4. The PSD alloys and Al-TM alloys clearly fall into two groups with the ratio $a_R/\bar{a} = 1.75$ and 1.65, respectively. The difference in the values of a_R/\bar{a} ($=1.75$) and a_R/\bar{d} ($=2.0$) for the PSD alloys may be partly attributed to overestimation of interatomic spacings of Mg and Li

atoms in crystalline compounds using the Goldschmidt diameters.

Experimentally observed icosahedral quasicrystals are found not to be perfectly quasiperiodic but can best be described by a random projection procedure,¹⁵ and by the so-called generalized dual method.¹⁶ The Hendrick-Teller disorder has been considered by Stephens and Goldman.¹⁷ This predicts that the peak broadening is a function of Q_\perp and should go to zero as $Q_\perp \rightarrow 0$.¹⁸ This is distinguishable from the peak broadening caused by ordinary disorder, e.g., strains, dislocations, compositional fluctuations, etc., in which the peak width is a function of Q .

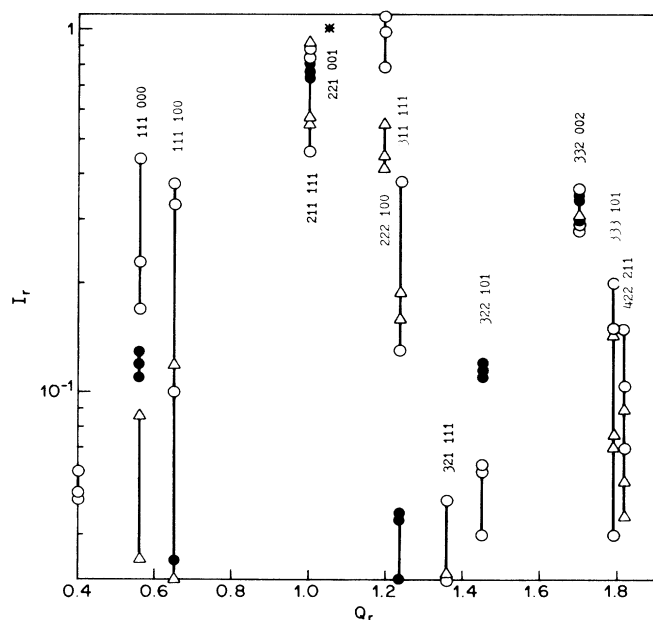


FIG. 3. Peak intensities $I_r(Q_r)$ of icosahedral quasicrystals. O, Li-based; Δ , Mg-based; and \bullet , Al-TM alloys.

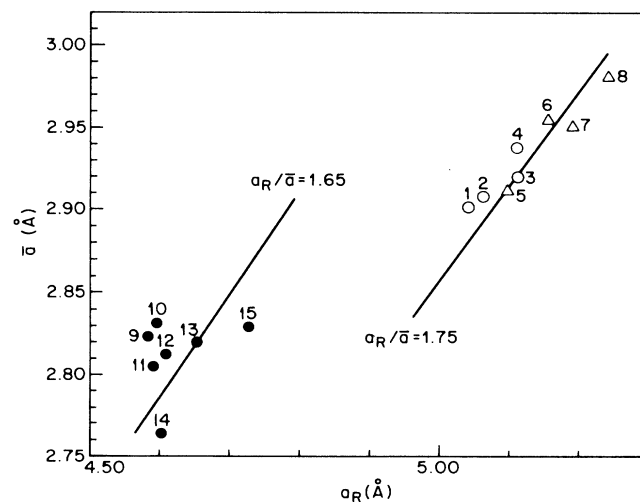


FIG. 4. The lattice parameter a_R plotted against the average Goldschmidt diameter \bar{a} for icosahedral crystals; (1) $\text{CuLi}_3\text{Al}_{5.9}$, (2) $\text{Au}_{0.2}\text{Cu}_{0.8}\text{Li}_3\text{Al}_6$, (3) AuLi_3Al_6 , (4) $\text{Zn}_{17}\text{Li}_{32}\text{Al}_{51}$, (5) $\text{Ga}_{16}\text{Mg}_{32}\text{Zn}_{52}$, (6) CuMg_4Al_6 , (7) $\text{Al}_2\text{Mg}_3\text{Zn}_3$, (8) $\text{Ag}_{15}\text{Mg}_{35}\text{Al}_{50}$, (9) $\text{Al}_{77.5}\text{Mn}_{22.5}$, (10) $\text{Al}_{82}\text{Mn}_{18}$, (11) $\text{Al}_{74}\text{Si}_6\text{Mn}_{15}\text{Fe}_5$, (12) $\text{Al}_{74}\text{Si}_6\text{Mn}_{20}$, (13) $\text{Al}_{84.5}\text{Cr}_{15.5}$, (14) $\text{Al}_{60}\text{Si}_{20}\text{Cr}_{20}$, and (15) $\text{Al}_{82.5}\text{V}_{17.5}$.

Here Q and Q_{\perp} are the three physical momenta and three orthogonal phason components of the six-dimensional reciprocal space in the projection techniques. As shown in Table I, the icosahedral crystals exhibit diffraction peak widths which are much broader than the instrumental resolution of $\sim 2.3 \times 10^{-3} \text{ \AA}^{-1}$, indicating the presence of considerable disorder. The half width at half maximum ΔQ ranges from 0.6×10^{-2} to $3.7 \times 10^{-2} \text{ \AA}^{-1}$, and thus the correlation length of structural order; $L \approx 2\pi/\Delta Q \leq 1000 \text{ \AA}$. The peak width broadening is larger in Mg-containing alloys than in the Li-based alloys. The i -CuLi₃Al_{5,9} shows the least peak width broadening.

We have found new quasicrystals in melt-spun Zn₁₇Li₃₂Al₅₁, Ga₁₆Mg₃₂Zn₅₂, Ag₁₅Mg₃₅Al₅₀, and AuLi₃Al₆ ribbon alloys. Of the new alloys found, three (Zn-Li-Al, Ga-Mg-Zn, and Ag-Mg-Al) are in the predictions listed (Ref. 20) in Ref. 5; the Au-Li-Al is not. We have found also that a number of alloys, such as AgLi₃Al₆, Au₁₅Mg₃₅Al₅₀, and Ag₁₅Mg₃₅Ge₅₀, which are

predicted in Ref. 5, do not form quasicrystal; the Au-Mg-Al and Ag-Mg-Ge are amorphous, while the Ag-Li-Al forms the R phase. However, to obtain stable quasicrystals these compositions must be fine tuned. We have found that even the stable CuLi₃Al₆ quasicrystal does not grow from a melt congruently and the i phase had to be obtained by casting the melt at moderate cooling rates to suppress the formation of the R phase. The present results are promising and they demonstrate the capability of quantum structural diagrams both for describing and predicting complex ternary alloy structure. The similarity in x-ray peak intensities and the packing densities as indicated by $a_R/\bar{a} \approx 1.75$ of the PSD quasicrystal family suggest similar atomic decoration of the rhombohedral unit cells of 3DPT. This atomic decoration is different from that of Al-TM alloys. It is interesting to note that the most stable CuLi₃Al₆ quasicrystal exhibits the least peak width broadening and structural disorder regardless of the quenching process.

*Permanent address: Villars Intermetallic Phases Data Bank, Postfach, CH-5628 Aristau, Switzerland.

†Permanent address: Research Institute for Iron, Steel, and Other Metals, Tohoku University, Sendai 980, Japan.

¹D. Schechtman, I. Bleck, D. Gratias, and J. W. Cahn, Phys. Rev. Lett. **53**, 1951 (1984).

²H. K. Hardy and J. M. Silcock, J. Inst. Met. **24**, 423 (1955).

³M. D. Ball and D. J. Lloyd, Scr. Metall. **19**, 1065 (1985); A. Sainfort and B. Dubost, J. Phys. (Paris) Colloq. **47**, C3-321 (1986); W. A. Casada, G. J. Shifflet, and S. J. Poon, Phys. Rev. Lett. **56**, 2276 (1986); C. Bartges, M. H. Tosten, P. R. Howell, and E. R. Ryba (unpublished); A. R. Kortan, H. S. Chen, and J. V. Waszczak (unpublished).

⁴V. Elser and C. L. Henley, Phys. Rev. Lett. **55**, 2883 (1985); P. Guyot and M. Audier, Philos. Mag. B **52**, L15 (1985); P. Ramachandrarao and G. V. S. Sastry, Pramana **25**, L225 (1985).

⁵P. Villars, J. C. Phillips, and H. S. Chen, Phys. Rev. Lett. **57**, 3085 (1986).

⁶D. C. Koskenmaki, H. S. Chen, and K. V. Rao, Phys. Rev. B **33**, 5328 (1986).

⁷D. C. Koskenmaki, H. S. Chen, and K. V. Rao, Scr. Metall. **20**, 1631 (1986).

⁸H. S. Chen and A. Inoue, Scr. Metall. **21**, 527 (1987).

⁹V. Elser, Phys. Rev. B **32**, 4892 (1985).

¹⁰H. S. Chen, A. R. Kortan, and J. Parsey (unpublished).

¹¹The strongest peak is at 221001 instead of 211111 observed previously for i -AlMn binary alloys.

¹²K. M. Knowles and W. M. Stobbs, Nature (London) **323**, 313 (1986).

¹³C. L. Henley and V. Elser, Philos. Mag. **53**, L59 (1986).

¹⁴A. Inoue, H. Kimura, and T. Masumoto (unpublished).

¹⁵P. Bak, Phys. Rev. Lett. **56**, 861 (1986).

¹⁶J. E. S. Socolar, P. J. Steinhardt, and D. Levine, Phys. Rev. B **32**, 5547 (1985).

¹⁷P. W. Stephens and A. I. Goldman, Phys. Rev. Lett. **56**, 1168 (1986).

¹⁸T. C. Lubensky, J. E. S. Socolar, P. J. Steinhardt, P. A. Bancel, and P. A. Heiney, Phys. Rev. Lett. **57**, 1440 (1986); P. M. Horn, W. Malzfeldt, D. P. DiVincenzo, J. Toner, and R. Gambino, *ibid.* **57**, 1444 (1986).

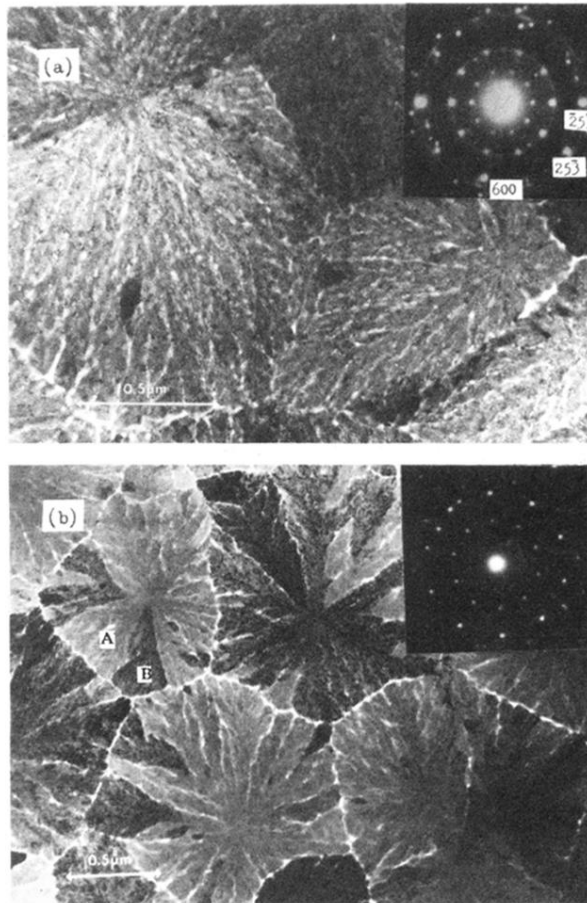


FIG. 1. Transmission electron microscope micrographs and diffraction patterns along fivefold axis of (a) AuLi₃Al₆ and (b) Ag₁₅Mg₃₅Al₅₀.